ISSN: 2835-7329

Research Article

Dermatology Journal of Cosmetic and Laser Therapy

Modelling and Quantifying The Impact of Photobiomodulation (PBM) on Biological Processes Relevant to Lymphangiogenesis, Anti-Inflammation, and Tissue Regeneration Processes: Results from a Meta-Analysis and a Neural Network Modelling

Abdullah Jibawi*

Ashford and St Peter's Hospital NHS Foundation Trust Chertsey, Surrey, United Kingdom, KT16 0PZ

***Corresponding Author**
Ashford and St Peter's Hospital NHS Foundation Trust Chertsey, Surrey, United Kingdom, KT16 0PZ

Submitted: 2023, Dec 13; **Accepted:** 2024, Jan 02; **Published:** 2024, Jan 11

Citation: Jibawi, A. (2024). Modelling and Quantifying The Impact of Photobiomodulation (PBM) on Biological Processes Relevant to Lymphangiogenesis, Anti-Inflammation, and Tissue Regeneration Processes: Results from a Meta-Analysis and a Neural Network Modelling. *Dearma J Cosmetic Laser Therapy, 3*(1), 01-09.

1. Introduction

Lymphoedema is a common and debilitating condition characterized by partial or complete derangement in the draining capabilities of the lymphatic system. Due to the disruption of lymphatic drainage, the build-up of fluids, proteins and lipids in the interstitial space leads to substantial and progressive architectural alterations in the regional tissue, including the accumulation of adipose tissue and fibrosis. These changes are associated with a progressive inflammatory process [1,2]. The therapeutic potential of photobiomodulation (PBM) for lymphoedema has been demonstrated by various studies, but the existing literature is limited by the lack of rigorous and consistent high-level evidence to allow for conclusive recommendations. PBM has been demonstrated to be capable of modulating inflammatory processes, facilitating lymphatic fluid drainage, alleviating discomfort, and improving quality of life in lymphoedema patients [3-6].

Since PBM's impact on lymphoedema has thus far been difficult to quantify accurately, the use of PBM as a therapeutic modality has remained mostly separate from the pharmaceutical field. In that field, biomarkers, laboratory tests, and patient-reported outcomes, among other parameters, can all be used to gauge how new drugs are working (phase 1 to 3 trials) [7]. This established methodology allows quantification of the pharmaceutical effect using numerical tools such as the number needed to treat (NNT) and other metrics. A similar quantification of PBM, if feasible, can provide a greater understanding of the dose needed to treat and the duration of treatment required to obtain the desired clinical effect. In this context, we use the term 'effect' to refer to two distinct aspects. First, we refer to an 'enhancing effect' to reflect PBM's established role in promoting lymphangiogenesis. This involves the stimulation of new lymphatic vessel formation, which is essential for improving lymphatic drainage and thereby alleviating the symptoms of lymphoedema. Second, we refer to the 'control effect' to denote PBM's capacity to modulate inflammation, which includes the reduction of pro-inflammatory cytokines and the promotion of an anti-inflammatory environment in the affected tissues.

This work has been presented at the 3rd BASIC VASCULAR SCIENCE (BVS) meeting in Leiden, the Netherlands, and it was endorsed for publication.

1.1 Objectives

To conduct a modelling exercise using raw data from studies that compared the effects of PBM on biological tissues to those of a placebo, with the aim of quantifying the specific biological alterations observed in tissues frequently involved in the lymphoedema disease process.

2. Methods

We implemented a systematic approach in reviewing the literature to isolate studies that met our criteria for assessing the impact of PBM on lymphoedema-related biomarkers. This process began with a detailed examination of Zein et al.'s (2018) systematic review [8]. Our inclusion criteria for selecting studies from this review were two-fold:

- Relevance to lymphoedema pathophysiology: Studies were chosen based on their focus on tissues and processes implicated in lymphoedema, thereby ensuring that the biomarkers analyzed were directly relevant to the condition.
- Study Design Preference: A clear distinction was made between in vitro and in vivo studies. We preferred in vitro studies for their ability to allow controlled examination of PBM effects, hence providing clarity on the direct impact of PBM on cellular and molecular processes without the confounding factors present in in vivo studies.

These criteria guided our selection process, leading to the inclusion of 8 studies out of the original 34 in Zein et al.'s review [8].

2.1 Biomarker Selection and Measurement Standardization

The biomarkers chosen for our analysis were specifically selected due to their known contribution to lymphoedema pathophysiology. These markers, detailed in Table 1 of our article, were reassessed on a fundamental level.

component	Relation to lymphoedema pathophysiology/presentation
MACROPHAGES	contribute to the formation of fibrous tissue and inflammation in the affected limb. 15 For example, Ghanta et al showed that macrophage depletion after lymphoedema significantly increased fibrosis and accumulation of CD4+ cells and promoted Th2 differentiation while decreasing lymphatic transport capacity and VEGF-C expression. 15
Neural cells	regulating the fluid balance in the interstitial spaces and transmitting sensory information to the central nervous system.16 For example, Karlsen et al demonstrated that the levels of the neuropeptides substance P and calcitonin gene-related peptide were increased in Chy mice, which may contribute to the pain and hypersensitivity associated with lymphoedema. 16
Cortical neurons	regulating the sympathetic and parasympathetic nervous system that controls the lymph nodes and fluid balance in the body.17
Monocytes	contribute to the formation of fibrous tissue and immune system dysfunction18, 19
Myotubes	contributes to the impaired lymphatic drainage and decreased muscle contractions necessary for proper fluid transport.2
Fibroblasts	contributing to the formation of fibrotic tissue and producing extracellular matrix components that alter lymphatic function.20 21, 22
Muscle fibre strength	Can impair proper lymphatic flow and contribute to fluid accumulation and tissue swelling.23

Table 1: This table shows a list of biomarkers chosen in this study due to their contribution to one or more components of lymphedema pathophysiology.

Measurements obtained from the selected studies were subjected to rigorous standardization. This process involved raw data quantification followed by feature scaling, employing the mean normalization method (Table 2). Such normalization enabled us to effectively compare biomarker values across studies, thus allowing us to assess the aggregate impact of PBM on these markers.

Component	Molecule/function studied
Macrophages	IL6, Cox2, TNFa
Neural cells	Toxicity. measured as: viability against cobalt (CoCl2) toxin, viability against H2O2 toxin.
	Excessive ROS toxicity. measured as: mitochondrial ROS and cellular ROS production using a CellROX red dye and 665nm light
cortical Neurons (mouse)	Mitochondrial activity. measured as: mitochondrial ROS and cellular ROS production using a MitoSox red dye and 510/580nm light, intracellular NO production using a DAF-DM and nuclear Hoechst dye, metochondria membrane potential, intracellular calcium, intracellular ATP
MONOCYTE	M1 polarisation Cytokine: measured as: CCL2 cytokine activity, CXCL10 cytokine activity, TNF Alpha cytokine activity, mitochondria copy number, mitochondria biogenesis, Histones modification (acetylation AcH3 or AcH4 or trimethylation H3K4) - epigenetic regulation, CCL2 cytokine activity, CXCL10 cytokine activity, TNF Alpha cytokine activity, mitochondria copy number, mitochondria biogenesis, Histones modification (acetylation AcH3 or AcH4 or trimethylation H3K4) - epigenetic regulation
Macrophages	Activity measured using colorimetric assay to assess the ability of mitochondrial enzyme succinate dehydrogenase in viable cells to cleave MTT in Macrophages J774
MYOTUBE_C2C12	Activity measured as: Metochondrial membrane potential based on illumination of TMRM flourecence, Metochondrial ATP content based on illumination of Promega flourecence
fibroblast	Human_fibroblast_enhanced_activity: expressed as fibroblast cell number, activation of cell proliferation gene (MAPK11, p38Beta2, BCR, PDGFC/VGEF, SRF, DAG 1), deactivation of cell suppression gene Cullin1, activation of antioxidant-related gene (SEPW1, ATOX2), deactivation of apoptosis gene (HSPA1A, CASP6), deactivation of apoptosis gene STIP1, activation of apoptosis gene (RIPK1, SSI-1), Human_fibroblast_protein_activity: expressed as effect on genes (CANX, ZMPSTE24, BCAT2, AHCY, TORIB, PSMB3, PPIH, ELL2, CCT2, PAMCI, HDLBP, ANPEP, ENO3, ALDOA, APOC3, LYPLA2, NR2F2, NDUFB2, ETFB), Human_fibroblast_energy_activity: expressed as effect on gene ATP5H, Human_fibroblast_ion_channel_activity: expressed as effect on genes (ABC1, KCNG1, SCN4A, KCNJ13, CLIC4, ASNA1), Human_fibroblast_Immune_activity: expressed as effect on genes (LENGS, AMSH, TSN, SEP2, ELF1).

muscle	Human_fibroblast_cytoskeleton_activity: expressed as effect on genes (DAG1, ARHD, MYH9, RANBP9, ARPC2, LRRFIP1, TPM4, KRTHA1), Human_fibroblast_exttacellular_matrix_activity: expressed as effect on genes (FMOD, TIP39, FBN1, MMP10), Human_fibroblast_migration_and_adhesion_activity: expressed as effect on genes (CEACAM3, CDH12, OC81537, ADRM1, CDH13), Human_fibroblast_DNA_Synthesis_and_repair_activity: expressed as effect on gene (MPG, APRT, NUDT1), Human_fibroblast_Transcription_factor_activity: expressed as effect on genes (GCN5L1, GAS41, LOC51131, ZNF74).

Table 2: A list of all Biological Components and Functions Analyzed and Activity Modelled in this Study

2.2 PBM and Placebo Arm Analysis

For every study included in our review, we extracted detailed PBM parameters for both the treatment and placebo arms. These parameters encompassed:

Body area targeted by PBM
PBM treatment frequency
Laser wavelength
Laser type
Duration of each PBM session
Total duration of PBM treatment
Treatment power settings
Irradiance and dosage
Intensity levels
Effect size and the timing of the observed effect

We obtained the exact measurements of each PBM and placebo arm, published in each article, and performed feature scaling to normalise the range of values measured using the mean normalisation method. This method rescaled the range of PBM values in percentage in relation to the control (sham) value using the formula:

$$x' = \frac{x - \mu}{\max(x) - \min(x)}$$

Normalization is a process used to convert numeric columns in a dataset to a common scale without losing differences in the ranges of values or information. This is done by subtracting the baseline value (u) from the original value (x) and then dividing by the baseline value (u), resulting in the normalized value (x'). For each measured point, the following PBM parameters were collected: body area treated with PBM, frequency of treatment, wavelength used, type of laser used, duration of treatment in each session, total time of treatment, treatment power, irradiance, dose, intensity, effect size and the timing of effect.

2.3 Statistical Analyses and Model Building

We implemented Bayesian linear regression to examine the relationship between PBM application timing and various PBM parameters in comparison to the placebo effect. This approach allowed for probabilistic interpretation of our findings and the integration of prior knowledge into our statistical inferences. For predictive modelling, we constructed a feedforward neural network (fNN) model. Our fNN model was designed with a specific architecture comprising seven hidden layers with 37 nodes each, aiming to capture the complex relationships between input parameters and the resulting biological effects of PBM.

The fNN was trained using a dataset randomly split into training (40%), validation (40%), and testing (20%) subsets. Logistic sigmoid functions were employed as activation functions within the network layers to introduce nonlinearity into the model. A genetic algorithm was utilized for optimization purposes, with a population size of 80 and running for 10 generations to fine-tune the model parameters. The performance of our fNN was analysed using the JASP Stat Package 0.16.3, providing valuable insights into the predictive accuracy of the model in terms of mean squared error (MSE) and coefficient of determination (R^2).

2.4 Ethical Considerations and Reproducibility

Importantly, our methodological approach was crafted with ethical considerations in mind. We only included data from studies that had obtained ethical clearance, and we conducted our review in accordance with the PRISMA guidelines to ensure the transparency and reproducibility of our research process. Moreover, our analytical approach and model-building efforts were meticulously documented, providing a clear path for other researchers to replicate or build upon our work. We believe that such rigorous methodology not only strengthens the validity of our findings but also encourages further advancements in the understanding and treatment of lymphoedema.

3. Results

We included 209 individual measurements from eight major comparative studies.

There is a clear pattern of multiple PBM activation phases over time, and this is quantifiable. We found that PBM therapy increased the average effect by 176.7% (standard error of mean: 9.6%) compared to placebo. The effect was much higher (75th percentile of 236% and a maximum of 850%) in the first phase (Table 3).

	Time_of_effect_h	degree_of_effect
Valid	209	209
Mode	8.0	125.0
Mean	10.6	176.7
Std. Error of Mean	1.3	9.6
Std. Deviation	18.2	138.2
Minimum	0.1	3.0
Maximum	120.0	850.0

Table 3: Descriptive values of measurements obtained when comparing PBM vs placebo

We used linear regression to investigate the relationship between the degree of the PBM effect and the timing of this effect, as well as various PBM parameters such as fluence, irradiance, energy, treated area, and duration (Figures 1, 2, and 3).

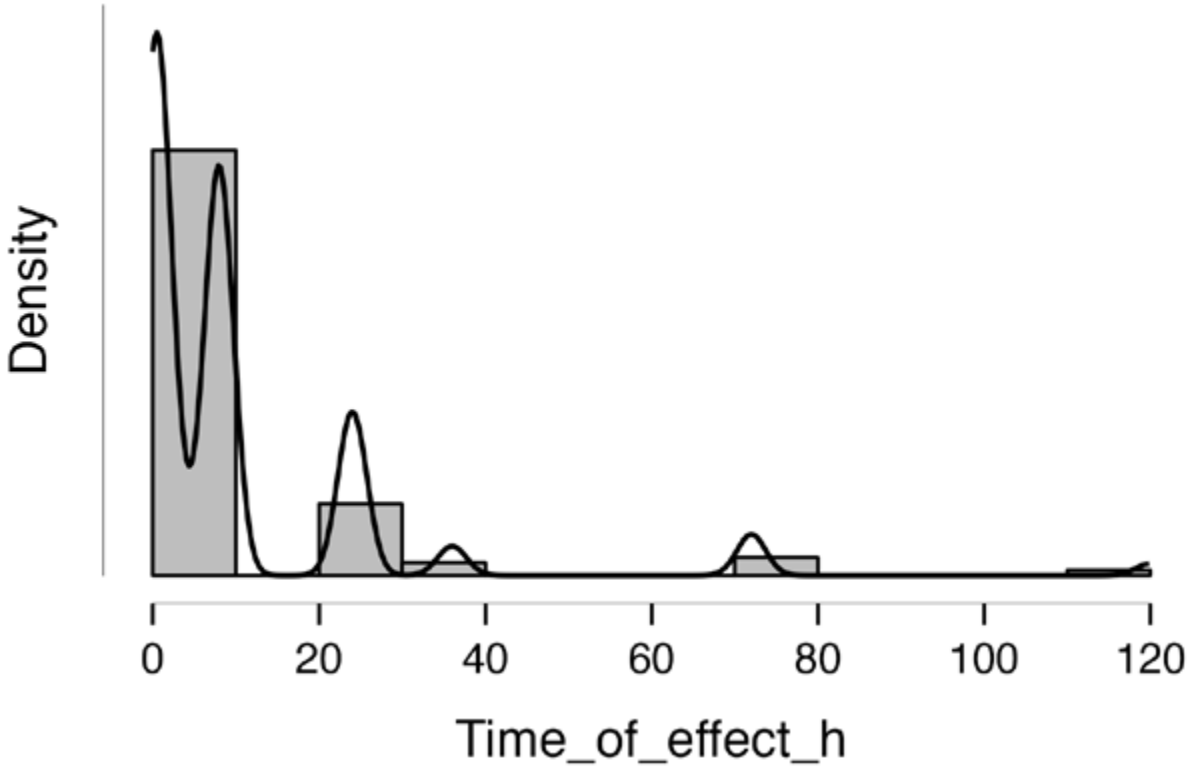

Figure 1: The figure shows the activation density of PBM over a period of time, with the initial density being the highest and decreasing gradually. The process goes through five distinct phases, each characterised by a different level of activation density. The process goes through five distinct phases, each characterised by a different level of activation density. The first phase starts with the highest density of activation, followed by a gradual decrease in the second phase and third phase. In the fourth phase, there is a slight increase in the activation density, which decreases further in the fifth and final phases over the studied period. Overall, the figure illustrates a pattern of multiphase activation with decreasing density over time.

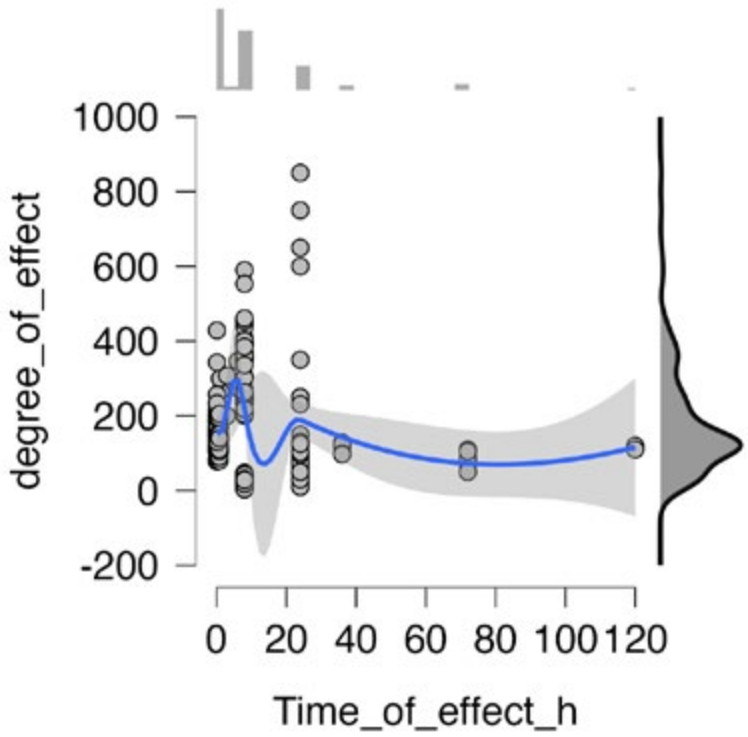

Figure 2: The figure displays a correlation between the time of effect of photobiomodulation (PBM) and the degree of effect. The correlation appears to be three-phasic, with the highest degree of effect observed within the first 10 hours. The graph shows a sharp increase in the degree of effect within the first 10 hours, followed by a second wave of effect that then decreases to increase to a lesser degree over time. The correlation suggests that the timing of observing the effect of PBM is an important factor in understanding its effectiveness. The graph also suggests that the initial response to PBM may be more pronounced than the long-term response.

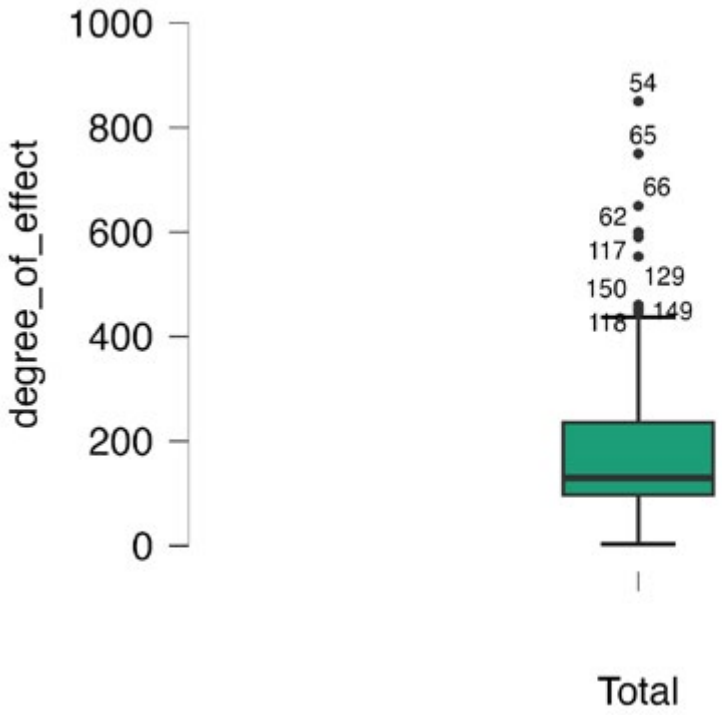

Figure 3: The box plot distribution chart displays the distribution of the effect of PBM, with the highest intensity clustered at approximately 175%. The chart shows that the intensity of the effect of PBM gradually increases from the lower quartile to the upper quartile, reaching a maximum of almost 850%. The interquartile range is relatively narrow, indicating a consistent distribution of the effect. The whiskers extend to the maximum and minimum values of the data, suggesting a few outliers at the higher end of the distribution. Overall, the box plot distribution chart illustrates a positively skewed distribution of the effect of PBM, with a large concentration of observations at a limited defined range, gradually increasing towards the upper end.

To assess the significance of our linear regression model, we performed an ANOVA. The resulting F-value was 3.8, with a corresponding p-value of <0.001. A large F-value indicates a stronger relationship between the independent variables (PBM timing) and the dependent variable (PBM standardised effect degree) (Table 4).

ANOVA

Model		Sum of Squares	df	Mean Square	F	p
H_1	Regression	465508.1	6	77584.7	3.8	1.4×10^{-3}
	Residual	$3.3\times10^{+6}$	161	20410.9		
	Total	$3.8\times10^{+6}$	167			

Note. The intercept model is omitted, as no meaningful information can be shown.

Table 4: ANOVA statistical results to test whether there was a significant difference in the degree of PBM effect among different levels of these features. The linear regression model showed an F-value of 3.8 and a p-value of <0.001.

A low p-value (<0.001) indicates that the probability of obtaining an F-value as large or larger than 3.8 by chance alone is very low. Therefore, we concluded that our linear regression model is statistically significant and that there is a significant relationship between the PBM parameters and the degree and timing of the PBM effect (figure 4).

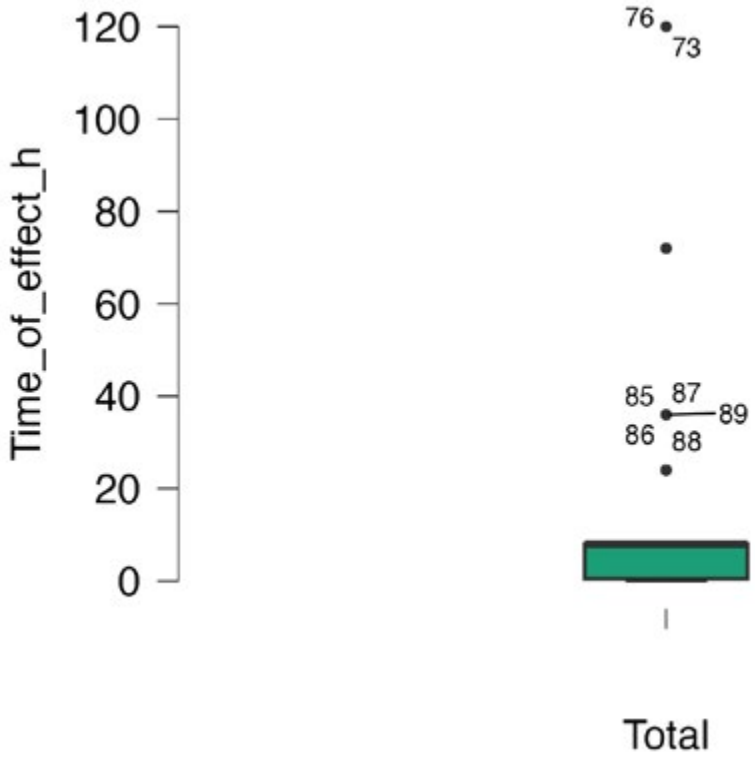

Figure 4: The box plot distribution chart represents the distribution of the time taken for PBM (photobiomodulation) to have its effect. The chart shows that the majority of the effects occurred after approximately 10 hours, with the interquartile range being relatively narrow, indicating a consistent distribution of the time taken for the PBM effect to manifest. The whiskers extend to the maximum and minimum values of the data, indicating that some observations took a longer time to exhibit the effect, with the maximum time being approximately 120 hours.

We built a feedforward neural network (fNN) with seven hidden layers and 37 nodes (Table 5 and Figure 5). The fNN model achieved an average mean squared error (MSE) of 1.232 and an average coefficient of determination (R2) of 0.081 on the test set. This means that our neural network regression model, with our chosen parameters, can explain 81% of the variance in the predictions (Table 6). The model performance was consistent across different PBM effects and PBM parameters.

Hidden Layers	Nodes	n(Train)	n(Validation)	n(Test)	Validation MSE	Test MSE
7	37	100	68	41	1.0	1.2

Note. The model is optimized with respect to the validation set mean squared error .

Table 5: This table presents a summary of the model's performance with information on the number of hidden layers, total number of nodes in the network, and number of observations in the training and test sets.

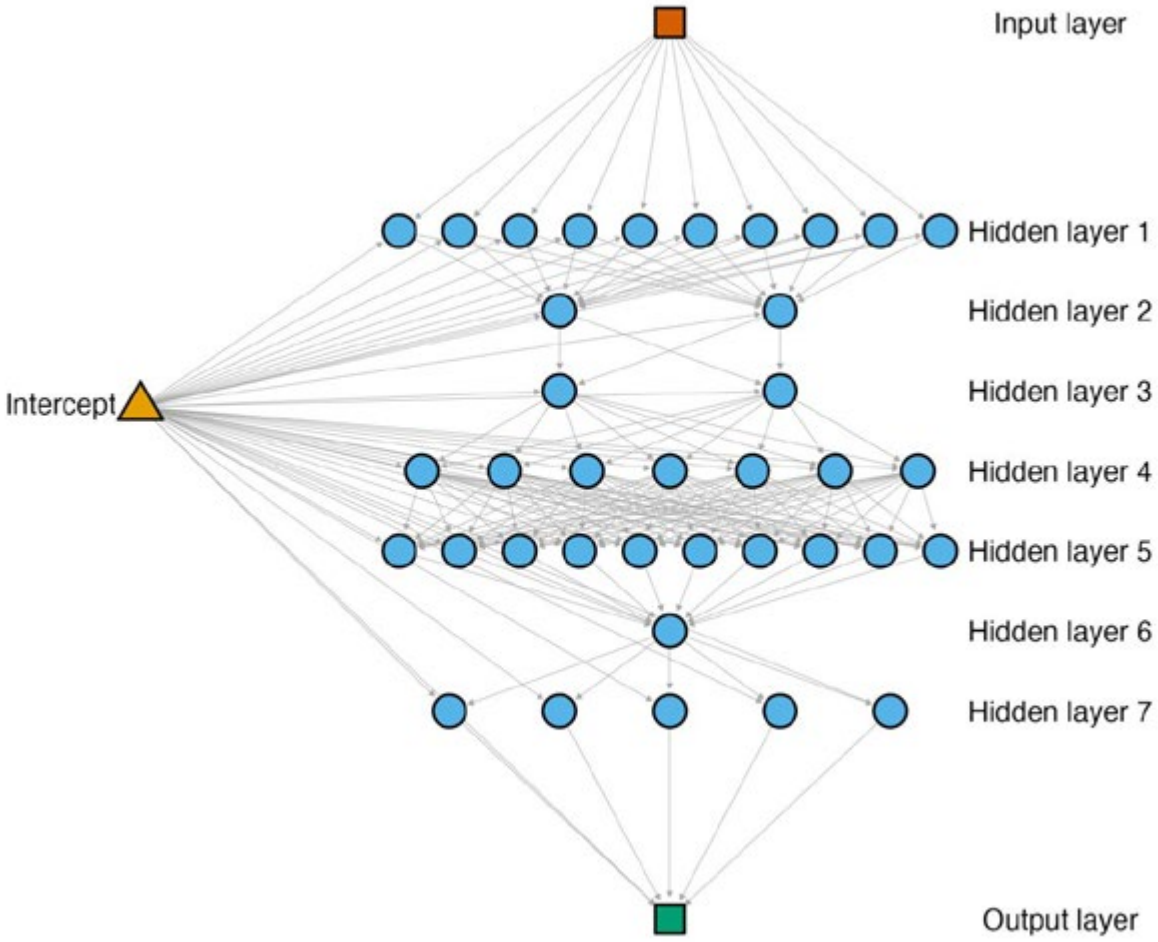

Figure 5: Network Structure Plot. This plot depicts the architecture of the neural network model used in this study. The model consists of an input layer, seven hidden layers, an output layer, and intercepts. The plot provides a visual representation of the model's complexity, which is important for understanding the model's ability to capture the underlying relationships between the input and output variables.

Evaluation Metrics	
	Value
MSE	1.232
RMSE	1.11
MAE / MAD	0.767
MAPE	108.14%
R^2	0.081

Table 6: The table provides a summary of the performance metrics for the model. The mean squared error (MSE) measures the average squared difference between the predicted and actual values.

These metrics show that the fNN could learn the input-output relationship well and make accurate predictions.

4. Discussion

Our research introduces new, rather novel, insights into the degree of activation achieved by photobiomodulation (PBM) when compared to placebo treatments using a new standardisation method and modelling. Prior studies have alluded to the activation potential of PBM, yet what distinguishes our work is the precise quantification of this impact [9]. This precision brings a

fresh perspective to the existing body of literature, promoting a deeper understanding of PBM's intrinsic mechanisms that align with pathways implicated in lymphoedema onset [1,2,10,11]. Building on this foundation, we refined our focus by narrowing the scope of the studies we analysed. Unlike the comprehensive set of studies in the Zein et al. (2018) review, our study intentionally focused on in vitro studies directly related to tissues impacted by lymphoedema [8]. This deliberate focus facilitated a nuanced understanding. We were able to define the 'effect' of PBM in terms of its 'enhancing effect' on lymphangiogenesis, as evidenced by heightened expression of lymphatic endothelial markers and the emergence of new lymphatic vessels. In parallel, the 'control effect' on inflammation was discerned through markers indicating decreased inflammation following PBM treatment.

Building on these molecular-level findings, we ventured into the application realm. We employed standardization techniques synonymous with deep learning to measure PBM effects, showcasing the adaptability of such methods beyond conventional contexts23, 24. This approach underscores a significant aspect of our research: not just understanding the biological underpinnings but establishing a quantifiable framework beneficial for clinicians. However, the diversity of PBM parameters reported presents a conundrum, pointing to the need for more encompassing meta-analyses to craft a precise model. Here, we see the potential of innovative neural network models, which could address these multifaceted challenges. However, our research, while foundational, comes with inherent limitations. Two main constraints were the finite pool of data measurements and the scope of molecules considered in lymphoedema pathogenesis. To truly advance our understanding, these limitations must be addressed in future research with a broader scope, capturing a wider array of measurements and parameters.

Transitioning from these foundational findings, we recognise the need to translate molecular-level insights to actionable clinical outcomes. Randomized trials have underscored the therapeutic potential of PBM, with tangible improvements noted in patient's posttreatment.3, 25 An exciting prospect for future research lies in bridging the gap between PBM's molecular effects, intricate biological processes, and ultimate clinical outcomes. By diving deep into this nexus, we can pave the way for personalized PBM treatment protocols, ensuring an amalgamation of molecular mechanisms, treatment intricacies, and patient benefits. In essence, our study, while a new potential cornerstone, sets the stage for expansive research that can truly revolutionize PBM's role in lymphoedema treatment [12-23].

Declarations

Ethical Approval

Not applicable

Competing interests

No competing interests of a financial or personal nature

Funding

No funding received

Availability of data and materials

No Data associated in the manuscript.

References

1. Azhar, S. H., Lim, H. Y., Tan, B. K., & Angeli, V. (2020). The unresolved pathophysiology of lymphedema. Frontiers in physiology, 11, 137.
2. Grada, A. A., & Phillips, T. J. (2017). Lymphedema: Pathophysiology and clinical manifestations. Journal of the American Academy of Dermatology, 77(6), 1009-1020.
3. Yilmaz, S. S., & Ayhan, F. F. (2023). The randomized controlled study of low-level laser therapy, Kinesio-taping and manual lymphatic drainage in patients with stage II breast cancer-related lymphedema. European Journal of Breast Health, 19(1), 34.
4. Kozanoglu, E., Gokcen, N., Basaran, S., & Paydas, S. (2022). Long-Term Effectiveness of Combined Intermittent Pneumatic Compression Plus Low-Level Laser Therapy in Patients with Postmastectomy Lymphedema: A Randomized Controlled Trial. Lymphatic Research and Biology, 20(2), 175-184.
5. Mahmood, D., Ahmad, A., Sharif, F., & Arslan, S. A. (2022). Clinical application of low-level laser therapy (Photo-biomodulation therapy) in the management of breast cancer-related lymphedema: a systematic review. BMC cancer, 22(1), 937.
6. Baxter, G. D., Liu, L., Petrich, S., Gisselman, A. S., Chapple, C., Anders, J. J., & Tumilty, S. (2017). Low level laser therapy (Photobiomodulation therapy) for breast cancer-related lymphedema: a systematic review. BMC cancer, 17(1), 1-13.
7. Ruberg, S. J., Harrell Jr, F. E., Gamalo-Siebers, M., LaVange, L., Jack Lee, J., Price, K., & Peck, C. (2019). Inference and decision making for 21st-century drug development and approval. The American Statistician, 73(sup1), 319-327.
8. Zein, R., Selting, W., & Hamblin, M. R. (2018). Review of light parameters and photobiomodulation efficacy: dive into complexity. Journal of biomedical optics, 23(12), 120901-120901.
9. Kataru, R. P., Baik, J. E., Park, H. J., Wiser, I., Rehal, S., Shin, J. Y., & Mehrara, B. J. (2019). Regulation of immune function by the lymphatic system in lymphedema. Frontiers in immunology, 10, 470.
10. Hohn, J., Tan, W., Carver, A., Barrett, H., & Carver, W. (2021). Roles of exosomes in cardiac fibroblast activation and fibrosis. Cells, 10(11), 2933.
11. Eckes, B., Kessler, D., Aumailley, M., & Krieg, T. (2000, June). Interactions of fibroblasts with the extracellular matrix: implications for the understanding of fibrosis. In Springer seminars in immunopathology (Vol. 21, pp. 415-429). Springer-Verlag.
12. de Brito, A. A., Gonçalves Santos, T., Herculano, K. Z., Estefano-Alves, C., de Alvarenga Nascimento, C. R., Rigonato-Oliveira, N. C., ... & Ligeiro de Oliveira, A. P. (2022). Photobiomodulation therapy restores IL-10 secretion in a murine model of chronic asthma: Relevance to the population of CD4+ CD25+ Foxp3+ Cells in lung. Frontiers in Immunology, 12, 789426.

13. Walski, T., Dąbrowska, K., Drohomirecka, A., Jędruchniewicz, N., Trochanowska-Pauk, N., Witkiewicz, W., & Komorowska, M. (2019). The effect of red-to-near-infrared (R/NIR) irradiation on inflammatory processes. International Journal of Radiation Biology, 95(9), 1326-1336.
14. Hamblin, M. R. (2017). Mechanisms and applications of the anti-inflammatory effects of photobiomodulation. AIMS biophysics, 4(3), 337.
15. Nie, F., Hao, S., Ji, Y., Zhang, Y., Sun, H., Will, M., ... & Ding, Y. (2023). Biphasic dose response in the anti-inflammation experiment of PBM. Lasers in Medical Science, 38(1), 66.
16. AlQuraishi, M., & Sorger, P. K. (2021). Differentiable biology: using deep learning for biophysics-based and data-driven modeling of molecular mechanisms. Nature methods, 18(10), 1169-1180.
17. Ching, T., Himmelstein, D. S., Beaulieu-Jones, B. K., Kalinin, A. A., Do, B. T., Way, G. P., ... & Greene, C. S. (2018). Opportunities and obstacles for deep learning in biology and medicine. Journal of The Royal Society Interface, 15(141), 20170387.
18. Ghanta, S., Cuzzone, D. A., Torrisi, J. S., Albano, N. J., Joseph, W. J., Savetsky, I. L., ... & Mehrara, B. J. (2015). Regulation of inflammation and fibrosis by macrophages in lymphedema. American Journal of Physiology-Heart and Circulatory Physiology, 308(9), H1065-H1077.
19. Karlsen, T. V., Karkkainen, M. J., Alitalo, K., & Wiig, H. (2006). Transcapillary fluid balance consequences of missing initial lymphatics studied in a mouse model of primary lymphoedema. The Journal of physiology, 574(2), 583-596.
20. Giron Jr, L. T., Crutcher, K. A., & Davis, J. N. (1980). Lymph nodes—a possible site for sympathetic neuronal regulation of immune responses. Annals of Neurology: Official Journal of the American Neurological Association and the Child Neurology Society, 8(5), 520-525.
21. Dayan, J. H., Ly, C. L., Kataru, R. P., & Mehrara, B. J. (2018). Lymphedema: pathogenesis and novel therapies. Annual review of medicine, 69, 263-276.
22. Eckes, B., Zigrino, P., Kessler, D., Holtkötter, O., Shephard, P., Mauch, C., & Krieg, T. (2000). Fibroblast-matrix interactions in wound healing and fibrosis. Matrix biology, 19(4), 325-332.
23. StatPearls. 2022.